Effect of different system parameters on the design of the EU DEMO Vacuum Vessel Pressure Suppression System

(Article begins on next page)

18 April 2024

Effect of different system parameters on the design of the EU DEMO Vacuum Vessel Pressure Suppression System

Antonio Froio [a,*], Ivo Moscato [b]

[a] NEMO group, Dipartimento Energia "Galileo Ferraris", Politecnico di Torino, Corso Duca degli Abruzzi, 24, 10129, Torino, Italy
[b] Fusion Technology Department, EUROfusion Consortium, Boltzmanstraße 2, 85748, Garching bei München, Germany

A B S T R A C T

The Vacuum Vessel Pressure Suppression System (VVPSS) is the safety system devoted to the mitigation of in-vessel Loss-Of-Coolant Accidents, which are considered among the Design-Basis Accidents for tokamak fusion reactors. The EUROfusion Consortium is performing the design of this system, as part of the conceptual design phase of the EU DEMO fusion reactor, including in the process its integration in the plant.

This work reports the first parametric calculations carried out to evaluate the VVPSS response to a postulated double-ended guillotine rupture of a Breeding Blanket coolant feeder. The aim of the study is to characterize the role that key parameters play on the multiple systems involved in such an accidental event. Assessments scanned a broad range of design variables, some closely related to the suppression system itself, and others dependent on Primary Heat Transfer System features. The parameter space is mapped identifying the regions where the accident consequences are fully mitigated, in terms of peak pressure in the Vacuum Vessel (VV) and equilibrium pressure of both VV and VVPSS, providing a design tool to rapidly adapt the VVPSS to the evolving plant design.

1. Introduction

The EU DEMO reactor [1] aims to become the first fusion device in the EU to produce fusion electricity, and is now facing its conceptual design phase by the EUROfusion Consortium [2–5], which includes the design of safety systems [6] such as the Vacuum Vessel Pressure Suppression System (VVPSS). The VVPSS is responsible for the mitigation of the consequences of accidents which would cause an overpressurization of the Vacuum Vessel (VV), which is the primary confinement barrier, and whose pressure limit is currently set to 2 bar, due to the presence of diamond windows in the gyrotron. One of such accidents is the in-vessel Loss-of-Coolant Accident (LOCA), caused when one of the Primary Heat Transfer Systems (PHTS) breaks releasing the coolant within the VV. Using passive systems such as Rupture Discs (RDs), the VVPSS extracts the coolant from the VV delivering it to an Expansion Volume (EV) [7].

The design of the VVPSS is based on the design-basis accident (DBA), which, among all the possible in-vessel LOCA scenarios, is the one featuring the harshest conditions, i.e. largest coolant inventory and largest break size. Therefore, the considered accident is a double-ended guillotine (DEG) break of a feeding pipe of the Breeding Blanket (BB) PHTS, namely the largest primary system, which is located in the upper port area.

The dimensioning of the VVPSS is thus strongly linked to that of other subsystems, mainly the BB-PHTS, but has also other constraints, related for instance to the space availability in the ports region or in the building. The aim of the present work is to analyse the effect of several parameters, directly related to either the VVPSS, or the PHTS, on the accidental transient following an in-vessel LOCA. The parametric scans are summarized in design maps, which then allow immediate evaluation of the acceptability of a given parameter combination, without the need to run detailed simulations.

The design maps are built by simulating all the possible combinations of the chosen parameters with a fast-running model, using the GEneral Tokamak THErmal-hydraulic Model (GETTHEM) [8], a tool developed at Politecnico di Torino with EUROfusion support for the transient thermal-hydraulic analysis of different subsystems relevant for the EU DEMO. The GETTHEM code has been successfully applied in the past for VVPSS-relevant analyses [9,10], and has been recently benchmarked against other tools such as CONSEN, MELCOR, and RELAP5-3D [11].

The paper is organized as follows: in Section 2, a brief description of the scenario, parameters, and model, is reported; then, the main results are summarized in Section 3; finally, the conclusions and future perspectives are described in Section 4.

---

2. Scenario and model description

In this section, the current design of the EU DEMO VVPSS (2.1), the investigated parameter space (2.2), and the relative GETTHEM model (2.3) are reported.

2.1. The EU DEMO VVPSS

The current layout of the EU DEMO VVPSS is sketched in Fig. 1. The connection of the VVPSS to the VV is routed via the upper port; this allows rapid mitigation of the transient when the DEG break happens in the upper port itself (as in the DBA under consideration here), while still being effective in case of leakages or ruptures in other locations [11]. At the same time, this location minimizes the space occupation, considering the presence of additional equipment at the lower (divertor PHTS, vacuum pumping) and equatorial (additional heating and current drive) ports.

The connection between the VV and the EV is achieved through a set of four DN800 pipes in parallel called Relief Lines (RL), each of which is equipped with a RD and a Bleed Valve (BV). The RD is passive, whereas the BV is an active valve with a smaller cross section, to be operated in case of small leakages, avoiding the burst of the RD which would require the intervention of the Remote Maintenance system to be replaced. The RD are set to open when a differential pressure of 1.5 bar develops across its surfaces. In the present work BVs are not considered because the small cross section and actuation time would make their effect marginal for the majority of the investigated transients.

The EV is constituted by five $500\,\text{m}^3$ tanks connected in series; to suppress the overpressurization, it is filled at 60% by liquid water, in sub-atmospheric conditions (and, in particular, at a pressure equal to the water saturation pressure at the given initial temperature): if the coolant to be discharged is also water, it will be in vapour phase, so the pressure will be reduced by condensing the steam; if instead the coolant is helium, there will still be a more effective pressure reduction by reducing its temperature. To this aim, other concepts, based on a passive heat exchanger, are being evaluated [7,12], but they are not considered in this work. A limit of 1.5 bar is currently set for the equilibrium pressure of the EV.

2.2. Investigated parameters

As mentioned in Section 1, some of the VVPSS design parameters are parametrically varied to analyse their effect on the transient evolution, within the limits allowed by the space constraints. In addition, also some of the PHTS design parameters are varied. These are:

- Number of VVPSS connection sets.
- Number of EV tanks.

Table 1
Parameter space.

Parameter	Value
Number of VVPSS connections	1 or 2 (×4×DN800)
Number of $500\,\text{m}^3$ EV tanks	3, 4, 5, or 10
Initial EV temperature	30 °C, 40 °C, 50 °C
Feeding pipe size	DN80 to DN350
PHTS volume	$100\,\text{m}^3$, $150\,\text{m}^3$, $200\,\text{m}^3$, …, $700\,\text{m}^3$

- Initial temperature of the EV tanks.
- Size of the PHTS feeding pipe.
- Coolant inventory in the PHTS (volume).

The first three parameters in the list above are VVPSS design parameters. Indeed, space may be available to route an additional set of four DN800 pipes from another upper port, and/or to introduce up to five additional tanks. On the other hand, the effect of a possible reduction of the number of tanks is considered. In addition, a sensitivity scan is performed on the EV initial temperature, starting from the "default" value of 30 °C, to evaluate what would be the impact of possibly higher temperatures.

The last two are PHTS design parameters. In principle, both of them are not free parameters, as they depend on the BB design, total power, and target efficiency. In particular, the feeding pipe size is determined based on the required mass flow rate, which in turn is correlated to the power to be removed; the PHTS volume instead depends on the size of the equipment (piping, circulators, pressurizers, etc.), which is again correlated to the total power. Nevertheless, both could be modified to some extent, without affecting the PHTS performance. The feeding pipe size may be reduced locally introducing smooth cross section restrictors, aiming at reducing the discharged mass flow rate during an accident. Indeed, in view of the large pressure difference between upstream (PHTS) and downstream (VV) the break, the flow will be choked, i.e. the velocity is limited by the speed of sound, so the total mass flow rate is directly proportional to the (smallest) cross-sectional area of the pipe. The PHTS volume may instead be reduced introducing or changing the PHTS segmentation in different loops, thus reducing the inventory which is released during an accident.

The parameter space explored in this work is reported in Table 1. Combining the different parameters, a total of 2496 cases are simulated. For the sake of these analyses, the BB is considered to be the Water-Cooled Lithium-Lead (WCLL) concept [13], which, being based on pressurized water (155 bar, 295 to 328 °C) [14,15], will present the most severe conditions for VVPSS dimensioning.

2.3. The GETTHEM model

The model used in the present analyses is based on that used in previous, similar works, which has been benchmarked [11] and, for the WCLL case, validated against experimental data [9].

The PHTS (and BB), the VV, and the EVs are modelled with a 0–D approach, i.e. the time-dependent mass and energy conservation equations are solved with a lumped model (ordinary differential equations), as well as the break (which is modelled as a valve) and the RDs. The RLs are instead modelled with a 1–D approach, solving the time-dependent mass, momentum, and energy conservation equations (partial differential equations); this enables a reliable calculation of the pressure drop in the RLs, which, if neglected, would cause an underestimation of the pressure peak in the VV. The BVs are not modelled in this work, as they have already been shown in the past not to play a significant role for large-break LOCAs [7], and also in view of their active nature; neglecting their role is a conservative approach, as the modelled cross section available for the coolant removal from the VV is smaller than the actual.

A sketch of the model is reported in Fig. 2. For further information on the model (implementation, verification, validation), please refer to [9,16].
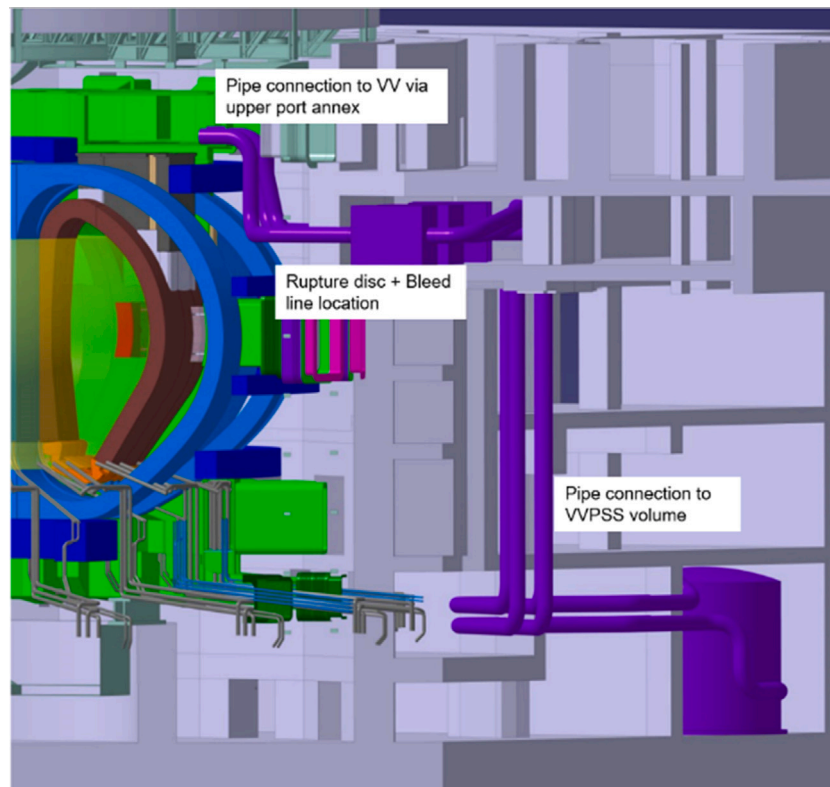
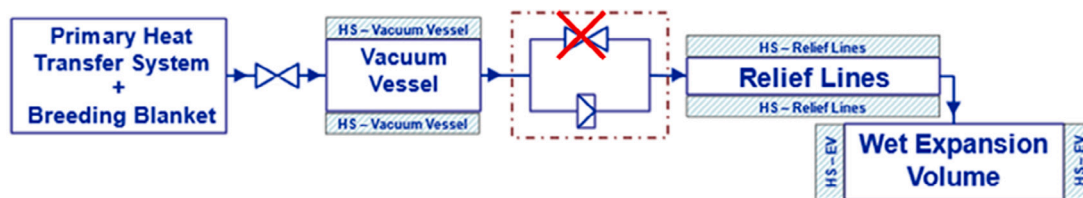**Fig. 1.** Preliminary model of the ducts connecting the VV to the VVPSS.

Fig. 2. Sketch of the model used in this work.
Source: Reproduced from [11].

3. Results

In view of the large amount of simulated scenarios, they are summarized in a set of 24 "design maps", one per each combination of VVPSS-related parameter (number of connection sets, number of EV tanks, initial EV temperature); each map is a 2-D table reporting on the horizontal axis the PHTS volume and on the vertical axis the feeding pipe size. These maps are available in [17]. The results of all the simulated scenarios, in terms of pressure evolution in the VV, can be qualitatively classified in three macro-cases, which are exemplified in Fig. 3: in the first one, the accident mitigation is so effective that the pressure in the VV starts decreasing as soon as the RDs intervene (Fig. 3(a)); in the second, the accident mitigation is still effective in keeping the VV pressure peak below the 2 bar limit, but the pressurization of the VV continues for a short time after the intervention of the RDs (Fig. 3(b)); in the last one, the accident mitigation is ineffective, causing the VV pressure to overcome the limit (Fig. 3(c)). These scenarios will be referred to as "green", "yellow", and "red", respectively, according to the colour code adopted in the design maps (see e.g. Tables 2 and 3).

In the following Section 3.1, the main, qualitative effect of each parameter is described. For given VVPSS parameters, the maps allow to identify all combinations of PHTS parameters (inventory and dimensions of feeding pipes) that ensure the verification of the safety limits.

From the maps, it is possible to derive the "limiting" scenarios for PHTS parameters (maximum inventory and maximum feeding pipe diameter). These "limiting" (i.e. maximum allowable) scenarios are summarized in Section 3.2.

3.1. Effect of the different parameters

As already evident from previous analyses [9–11], the main driver for the peak VV pressure is represented by the break size (or its ratio with respect to the total cross section available in the VVPSS connection pipes), whereas the PHTS volume (or its ratio with respect to the total EV volume) drives the equilibrium pressure. Indeed, a threshold-like behaviour is evident, in particular concerning the feeding pipe size, with all scenarios with pipes larger than DN150 (for one VVPSS connection set) or DN200 (for two VVPSS connection sets) causing the VV to over-pressurize, irrespectively of the PHTS inventory (with some small exceptions for very large inventories). Therefore, the VVPSS can suppress the pressure peak (below 2 bar) provided its total flow area is at least 120× larger than that of the feeding pipe (even though this figure should be taken as an indicative measure only, given that only pipe diameters according to the ISO 6708 standard have been considered in the present work). Similarly, the minimum required VVPSS volume to allocate all the PHTS inventory without overcoming
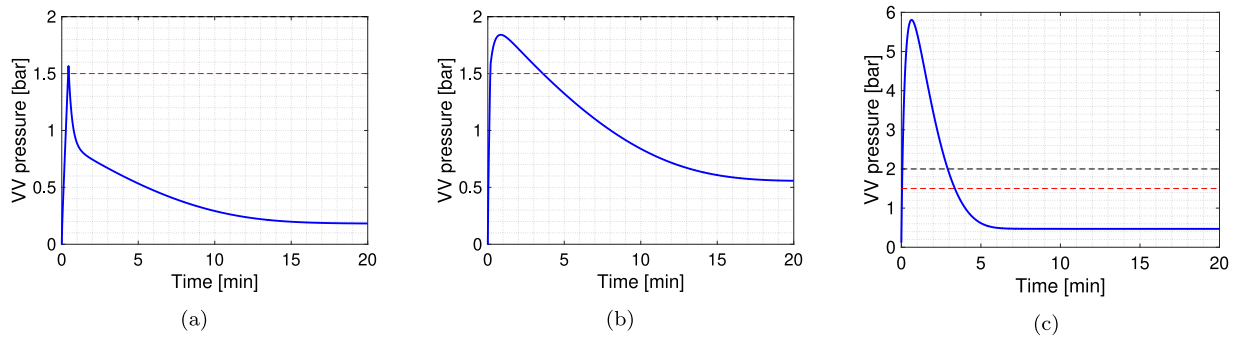
Fig. 3. Examples of evolution of the VV pressure, for (a) a "green" case, (b) a "yellow" case, and (c) a "red" case. The VV and EV pressure limits (2 bar and 1.5 bar) are shown with the thin dashed lines in black and red, respectively.

Table 2
Output matrix for initial EV temperature of 50 °C, 5 EV tanks, and one VVPSS connection set. The limiting scenario is in boldface and underlined.

p_{max} [bar]	Pipe DN	PHTS inventory [m³]												
		100	150	200	250	300	350	400	450	500	550	600	650	700
	80	1.616	1.616	1.616	1.616	1.616	1.616	1.616	1.616	1.616	1.616	1.616	1.616	1.616
	100	1.616	1.616	1.616	1.616	1.616	1.616	1.616	1.616	1.616	1.616	1.616	1.616	1.616
	125	1.616	1.616	1.616	1.616	1.616	1.616	1.616	1.616	1.616	1.616	1.616	1.662	1.786
	150	1.682	1.715	1.742	1.764	1.783	1.799	1.812	1.824	**_1.834_**	1.844	1.852	1.870	2.049
	200	2.515	2.643	2.739	2.815	2.877	2.928	2.972	3.010	3.042	3.071	3.097	3.120	3.141
	250	3.373	3.606	3.785	3.926	4.046	4.144	4.228	4.301	4.365	4.419	4.472	4.518	4.559
	300	4.138	4.490	4.761	4.981	5.162	5.316	5.449	5.564	5.666	5.757	5.839	5.901	5.980
	350	4.584	5.007	5.339	5.609	5.835	6.027	6.193	6.339	6.468	6.583	6.687	6.781	6.866

Table 3
Output matrix for initial EV temperature of 50 °C, 5 EV tanks, and two VVPSS connection sets. The limiting scenario is in boldface and underlined.

p_{max} [bar]	Pipe DN	PHTS inventory [m³]												
		100	150	200	250	300	350	400	450	500	550	600	650	700
	80	1.616	1.616	1.616	1.616	1.616	1.616	1.616	1.616	1.616	1.616	1.616	1.616	1.616
	100	1.616	1.616	1.616	1.616	1.616	1.616	1.616	1.616	1.616	1.616	1.616	1.616	1.616
	125	1.616	1.616	1.616	1.616	1.616	1.616	1.616	1.616	1.616	1.616	1.616	1.649	1.770
	150	1.616	1.616	1.616	1.616	1.616	1.616	1.616	1.616	1.616	1.616	1.690	1.867	2.045
	200	1.618	1.630	1.644	1.657	1.668	1.679	1.689	1.697	**_1.705_**	1.711	1.753	1.892	2.181
	250	2.130	2.216	2.281	2.332	2.373	2.408	2.437	2.462	2.484	2.504	2.521	2.536	2.550
	300	2.691	2.839	2.951	3.089	3.110	3.171	3.222	3.266	3.304	3.338	3.368	3.395	3.420
	350	3.305	3.226	3.370	3.484	3.578	3.656	3.723	3.781	3.831	3.876	3.915	3.951	3.982

the 1.5 bar limit ranges from 3.5× to 6× the PHTS volume, according to the EV temperature (lower is better).

Overall, the results highlight compatibility of the VVPSS (with two connection sets) with the WCLL BB PHTS at its current design stage, which foresees the use of DN200 pipes for the largest feeding pipes [15,18]; further segmentation of the PHTS (e.g. due to radioactive inventory concerns) might also lower this value to DN150.

This can be seen in the two maps reported in Table 2 and Table 3 for one and two VVPSS connection sets, respectively, and for the "default" scenario (five tanks), with conservative initial temperature of 50 °C: in the tables, a green background represents a scenario in which the maximum pressure $p_{max} < 1.8$ bar (i.e. the 2 bar limit, minus 10 % tolerance), a yellow background means $p_{max} < 2$ bar (i.e. within the limit), and a red background means $p_{max} > 2$ bar (i.e. beyond the limit); similarly, a green text means an equilibrium pressure $p_{eq} < 1.35$ bar (i.e. the 1.5 bar limit, minus 10 % tolerance), a yellow text means $p_{eq} < 1.5$ bar (i.e. within the limit), and a red text means $p_{eq} > 1.5$ bar (i.e. beyond the limit). It is thus evident how all the scenarios with feeding pipe up to DN150 can be suppressed by a VVPSS with one connection set, whereas the limit increases up to DN200, as mentioned above. At the same time, the maps highlights that the PHTS inventory drives (almost exclusively) the equilibrium pressure, which is unaffected by the number of VVPSS connection sets (as there is no difference between Tables 2 and 3 in this respect).

This behaviour is also reported in Fig. 4, which shows the variation of the maximum pressure as a function of the feeding pipe DN, PHTS inventory, number of VVPSS connection sets, and initial EV temperature. In addition to the effect of the feeding pipe size (and of the number of VVPSS connection sets), it shows the smaller but non-negligible effect of the initial EV temperature, which amplifies the effect of the larger PHTS inventories, reducing, in the worst cases, the maximum possible PHTS feeding pipe size for the same number of VVPSS connection sets. As an example, it is possible to compare Fig. 4(f) with Figs. 4(b) and 4(d): in the first, with the largest EV temperature (50 °C), for a PHTS inventory of 700 m³, the maximum possible feeding pipe size is reduced to DN125, as opposed to DN200 in the other two cases. Nevertheless, it should be highlighted that 50 °C is a quite overconservative assumption, and it still affects only the worst case scenario as far as the PHTS inventory is concerned.

3.2. Summary of "limiting" scenarios

For each combination of VVPSS-related parameters (number of tanks, number of connection sets, initial temperature), a "limiting"
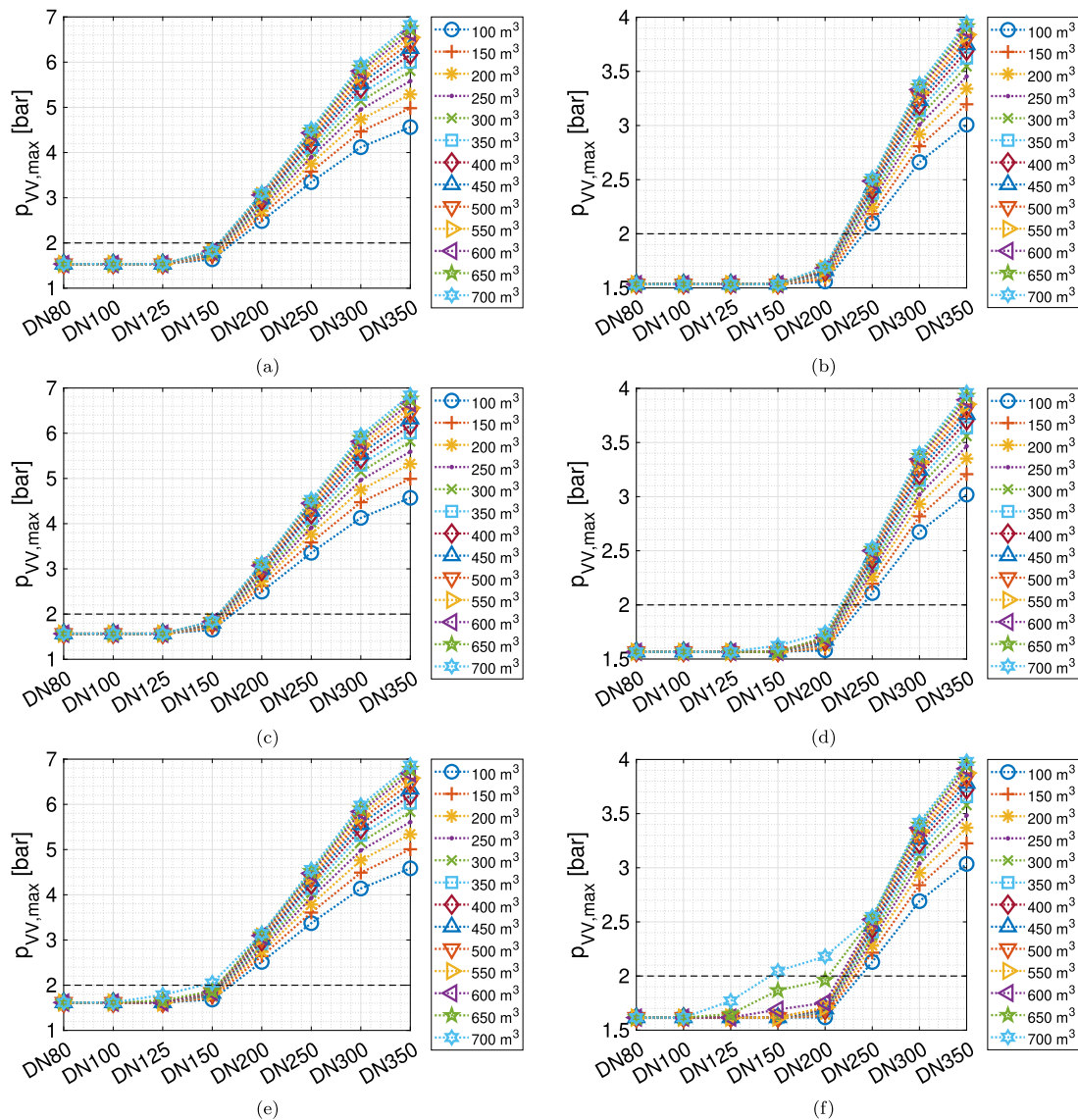
Fig. 4. Parametric effect of the feeding pipe DN on the peak pressure, for different PHTS volumes, with 5 EV tanks. (a): initial EV temperature 30 °C, one VVPSS connection set; (b): initial EV temperature 30 °C, two VVPSS connection sets; (c): initial EV temperature 40 °C, one VVPSS connection set; (d): initial EV temperature 40 °C, two VVPSS connection sets; (e): initial EV temperature 50 °C, one VVPSS connection set; (f): initial EV temperature 50 °C, two VVPSS connection sets. The VV pressure limit (2 bar) is shown with the black, thin, dashed line.

PHTS configuration can be identified looking at the maps such as those reported in Tables 2 and 3; in this work, this limiting configuration is chosen as the largest PHTS inventory which allows using the largest possible feeding pipe size: for instance, looking at Table 2, the largest possible feeding pipe size is DN150, thus the limiting PHTS configuration corresponds to the one with DN150 feeding pipes and 500 m³ inventory (as larger inventories would imply an equilibrium pressure above the limit). This does not take into consideration other, important PHTS design constraints, which are beyond the scope of the work, but that could be taken into consideration whilst moving in the "green" region of each map.

The limiting configuration for all the possible VVPSS designs considered in this work are reported in Table 4.

4. Conclusions and perspective

The GETTHEM model for an in-vessel LOCA in a water-cooled EU DEMO has been applied to perform a sensitivity analysis on different VVPSS and PHTS design parameters. The PHTS size, feeding pipe size, initial EV temperature, number of EV tanks, and number of VVPSS

connections have been varied, for a total of almost 2500 combinations, to identify the acceptable and unacceptable scenarios, for each possible VVPSS configuration. The analysis showed that the most relevant parameter is the ratio between the cross section of the feeding pipe (where the break occurs) and that of the VVPSS connection, which drives the most important differences in the outcome. Indeed, a threshold behaviour is visible for large feeding pipe sizes, but the maximum allowable diameter is DN150 if using one VVPSS connection set, and DN200 if using 2 VVPSS connection sets, which is compatible with the current PHTS design. The other parameter which plays a less-negligible role is the initial temperature, which however becomes significant only for larger PHTS volumes. All the results have been summarized in "design maps", which allow a rapid update of the VVPSS design given a change in the PHTS design (or vice-versa).

In perspective, the VVPSS design will be finalized in order to allow more detailed (verification-oriented) analyses to be carried out and fix the space occupation. Some improvements to the VVPSS design are also being considered, for example introducing a passive heat exchanger, which would reduce the energy content of the coolant before its expansion in the EV, thus reducing the required volume (and possibly further

Table 4
Limiting VVPSS configurations.

VVPSS design			Limiting PHTS configuration	
Temperature	Connections	Tanks	Feeding pipe diameter	Inventory
30 °C	1	3	DN150	400 m³
		4		550 m³
		5		>700 m³
		10		>700 m³
	2	3	DN200	400 m³
		4		550 m³
		5		>700 m³
		10		>700 m³
40 °C	1	3	DN150	350 m³
		4		450 m³
		5		600 m³
		10		>700 m³
	2	3	DN200	350 m³
		4		450 m³
		5		600 m³
		10		>700 m³
50 °C	1	3	DN150	250 m³
		4		400 m³
		5		500 m³
		10		>700 m³
	2	3	DN200	250 m³
		4		400 m³
		5		500 m³
		10		>700 m³

mitigating the transient); such solution is particularly interesting for the case of a non-condensable coolant, such as helium.

Declaration of competing interest

The authors declare that they have no known competing financial interests or personal relationships that could have appeared to influence the work reported in this paper.

Data availability

Data associated to the work is open and available at doi: https://doi.org/10.5281/zenodo.7094684.

References

[1] A.J.H. Donné, W. Morris, X. Litaudon, C. Hidalgo, D. McDonald, H. Zohm, E. Diegele, A. Möslang, K. Nordlund, G. Federici, P. Sonato, C. Waldon, D. Borba, P. Helander, European reasearch roadmap to the realisation of fusion energy, ISBN 978-3-00-061152-0, EUROfusion Consortium, 2018.

[2] G. Federici, J. Holden, C. Baylard, A. Beaumont, The EU DEMO staged design approach in the Pre-Concept Design Phase, Fusion Eng. Des. 173 (2021) 112959, http://dx.doi.org/10.1016/j.fusengdes.2021.112959, URL https://www.sciencedirect.com/science/article/pii/S0920379621007353.

[3] R. Kembleton, J. Morris, M. Siccinio, F. Maviglia, the PROCESS team, EU-DEMO design space exploration and design drivers, Fusion Eng. Des. 178 (2022) 113080, http://dx.doi.org/10.1016/j.fusengdes.2022.113080, URL https://www.sciencedirect.com/science/article/pii/S0920379622000801.

[4] R. Kembleton, C. Bustreo, Prospective research and development for fusion commercialisation, Fusion Eng. Des. 178 (2022) 113069, http://dx.doi.org/10.1016/j.fusengdes.2022.113069, URL https://www.sciencedirect.com/science/article/pii/S0920379622000692.

[5] G. Federici, C. Baylard, A. Beaumont, J. Holden, The plan forward for EU DEMO, Fusion Eng. Des. 173 (2021) 112960, http://dx.doi.org/10.1016/j.fusengdes.2021.112960, URL https://www.sciencedirect.com/science/article/pii/S0920379621007365.

[6] G. Caruso, S. Ciattaglia, B. Colling, L. Di Pace, D.L. Dongiovanni, M. D'Onorio, M. Garcia, X.Z. Jin, J. Johnston, D. Leichtle, T. Pinna, M.T. Porfiri, W. Raskob, N. Taylor, N. Terranova, R. Vale, all contributors to the WPSAE, DEMO – The main achievements of the Pre – Concept phase of the safety and environmental work package and the development of the GSSR, Fusion Eng. Des. 176 (2022) 113025, http://dx.doi.org/10.1016/j.fusengdes.2022.113025, URL https://www.sciencedirect.com/science/article/pii/S0920379622000254.

[7] G.A. Spagnuolo, R. Arredondo, L.V. Boccaccini, P. Chiovaro, S. Ciattaglia, F. Cismondi, M. Coleman, I. Cristescu, S. D'Amico, C. Day, A. Del Nevo, P.A. Di Maio, M. D'Onorio, G. Federici, F. Franza, A. Froio, C. Gliss, F.A. Hernández, A. Li Puma, C. Moreno, I. Moscato, P. Pereslavtsev, M.T. Porfiri, D. Rapisarda, M. Rieth, A. Santucci, J.C. Schwenzer, R. Stieglitz, S. Tosti, F. Roca Urgorri, M. Utili, E. Vallone, Integrated design of breeding blanket and ancillary systems related to the use of helium or water as a coolant and impact on the overall plant design, Fusion Eng. Des. 173 (2021) 112933, http://dx.doi.org/10.1016/j.fusengdes.2021.112933.

[8] A. Froio, F. Casella, F. Cismondi, A. Del Nevo, L. Savoldi, R. Zanino, Dynamic thermal-hydraulic modelling of the EU DEMO WCLL breeding blanket cooling loops, Fusion Eng. Des. 124 (2017) 887–891, http://dx.doi.org/10.1016/j.fusengdes.2017.01.062.

[9] A. Froio, A. Bertinetti, S. Ciattaglia, F. Cismondi, L. Savoldi, R. Zanino, Modelling an in-vessel loss of coolant accident in the EU DEMO WCLL breeding blanket with the GETTHEM code, Fusion Eng. Des. 136 (2018) 1226–1230, http://dx.doi.org/10.1016/j.fusengdes.2018.04.106.

[10] A. Froio, L. Barucca, S. Ciattaglia, F. Cismondi, L. Savoldi, R. Zanino, Analysis of the effects of primary heat transfer system isolation valves in case of in-vessel loss-of-coolant accidents in the EU DEMO, Fusion Eng. Des. 159 (2020) 111926, http://dx.doi.org/10.1016/j.fusengdes.2020.111926.

[11] M. D'Onorio, S. D'Amico, A. Froio, M.T. Porfiri, G.A. Spagnuolo, G. Caruso, Benchmark analysis of in-vacuum vessel LOCA scenarios for code-to-code comparison, Fusion Eng. Des. 173 (2021) 112938, http://dx.doi.org/10.1016/j.fusengdes.2021.112938.

[12] S. D'Amico, Integral approach to the safety design of the EU-DEMO Helium-Cooled Pebble Beds with reference to the associated relevant systems (Ph.D. thesis), Università degli Studi di Palermo, 2020.

[13] P. Arena, A. Del Nevo, F. Moro, S. Noce, R. Mozzillo, V. Imbriani, F. Giannetti, F. Edemetti, A. Froio, L. Savoldi, A. Tassone, F. Roca Urgorri, P.A. Di Maio, I. Catanzaro, G. Bongiovì, The DEMO Water-Cooled Lead-Lithium breeding blanket: Design status at the end of the pre-conceptual design phase, Appl. Sci. 11 (24) (2021) 11592, http://dx.doi.org/10.3390/app112411592.

[14] L. Barucca, W. Hering, S. Perez-Martin, E. Bubelis, A. Del Nevo, M. Di Prinzio, M. Caramello, A. D'Alessandro, A. Tarallo, E. Vallone, I. Moscato, A. Quartararo, S. D'Amico, F. Giannetti, P. Lorusso, V. Narcisi, C. Ciurluini, M.J. Montes Pita, M.C. Sánchez Naranjo, A. Rovira, D.J. Santana, P. Gonzales, R. Barbero Fresno, M. Zaupa, M. Szogradi, S. Normann, M. Vaananen, J. Ylatalo, M. Lewandowska, L. Malinowski, E. Martelli, A. Froio, P. Arena, A. Tincani, Maturation of critical technologies for the DEMO balance of plant systems, Fusion Eng. Des. 179 (2022) 113096, http://dx.doi.org/10.1016/j.fusengdes.2022.113096.

[15] I. Moscato, L. Barucca, E. Bubelis, G. Caruso, S. Ciattaglia, C. Ciurluini, A. Del Nevo, P.A. Di Maio, F. Giannetti, W. Hering, P. Lorusso, E. Martelli, V. Narcisi, S. Norrman, T. Pinna, S. Perez-Martin, A. Quartararo, M. Szogradi, A. Tarallo, E. Vallone, Tokamak cooling systems and power conversion system options, Fusion Eng. Des. 178 (2022) 113093, http://dx.doi.org/10.1016/j.fusengdes.2022.113093.

[16] A. Froio, Multi-scale thermal-hydraulic modelling for the Primary Heat Transfer System of a Tokamak (Ph.D. thesis), Politecnico di Torino, 2018, http://dx.doi.org/10.6092/polito/porto/2704378.

[17] A. Froio, Effect of different system parameters on the design of the EU DEMO vacuum vessel pressure suppression system (dataset), 2022, http://dx.doi.org/10.5281/zenodo.7094685, Zenodo.

[18] V. Narcisi, F. Giannetti, A. Del Nevo, WCLL BB PHTS architecture description & BOM (direct coupling option with small ESS), EFDA_D_2PC2N9, 2020.